AIE-Armored Living Bacteriophage-DNA Bioconjugates for Targeting, Imaging, and Efficiently Elimination of Intracellular Bacterial Infection

Jing Zhang[†], Xuewen He[†,*], and Ben Zhong Tang [Φ]

[†]The Key Lab of Health Chemistry and Molecular Diagnosis of Suzhou, College of Chemistry, Chemical Engineering and Materials Science, Soochow University, Suzhou 215123, China; Email: xheao@suda.edu.cn

[Φ]School of Science and Engineering, Shenzhen Institute of Aggregate Science and Technology, The Chinese University of Hong Kong, Shenzhen, Guangdong 518172, China; Email: tangbenz@cuhk.edu.cn

Abstract

Intracellular bacterial infections bring a considerable risk to human life and health due to their capacity to elude immune defenses and exhibit significant drug resistance. As a result, confronting and managing these infections presents substantial challenges. In this study, we developed a multifunctional phage bioconjugate by integrating aggregation-induced emission luminogen (AIEgen) photosensitizers and nucleic acid onto a bacteriophage framework (forming MS2-DNA-AIEgen bioconjugates). These bioconjugates can rapidly penetrate mammalian cells and specifically identify intracellular bacteria, while concurrently producing a detectable fluorescent signal. By harnessing the photodynamic properties of AIE photosensitizer and the bacteriophage's inherent lysis capability, the intracellular bacteria can be effectively eliminated and the functionality of the infected cells can be restored. In macrophage models infected with either antibiotic-sensitive or resistant *Escherichia coli*, MS2-DNA-AIEgen bioconjugates demonstrated excellent bacterial targeting and killing capability. Moreover, our engineered multifunctional phage bioconjugates were able to expedite the healing process in bacterially infected wounds observed in diabetic mice models while simultaneously enhancing immune activity within infected cells and in vivo, without displaying any noticeable toxicity. We envision that these innovative multifunctional phage bioconjugates, which utilize aggregation-induced luminescence photosensitizers and nucleic acids, may present a groundbreaking strategy for combating intracellular bacterial infections. This approach holds the potential to offer new avenues for future research and theranostic applications in the area of intracellular bacterial infections and associated diseases.

Keywords: bacteriophage, nucleic acid, antibacterial, aggregation-induced emission, photodynamic

Bacterial infections have long been a significant cause of severe illness and persistently high mortality rates worldwide.[1] The groundbreaking discovery of penicillin in 1928, followed by its clinical application, revolutionized antibiotic treatment and saved innumerable lives from bacterial infections.[2] However, the rampant abuse and overuse of these antibiotics have led to an increasingly dire issue of antibiotic resistance. It is projected that by 2050, 10 million people will perish annually as a result of antimicrobial resistance.[3] Even more alarmingly, certain bacteria can thrive and multiply within host cells, demonstrating significant resistance to conventional antibiotic treatments.[4-6] These intracellular bacteria, when not entirely eliminated, can spread from the initial site of infection to other tissues, leading to chronic or recurring infections.[7] Although immune cells, such as macrophages, play a crucial role in defending against bacterial infections by identifying, engulfing, and breaking down invasive bacterial pathogens, certain intracellular bacteria possess specialized secretion systems that enable them to survive within macrophages.[8] In such situations, macrophages not only fail to eliminate the bacteria but may inadvertently facilitate bacterial propagation. As these infected macrophages transport the pathogens throughout the body, they can cause severe diseases, such as tuberculosis, septicemia, dysentery, and epidemic cerebrospinal meningitis, among others. This hijacking of the immune system's normal defense mechanisms contributes to the persistence and spread of these infections, making them particularly challenging to treat.[9,10] In addition, the protective barrier created by host macrophages significantly impedes the identification and elimination of intracellular bacteria.[11] Moreover, mounting evidence indicates that intracellular bacteria are intricately linked to the onset and progression of malignant diseases. For instance, the existence of bacteria within tumors has been found to potentially foster resistance to cancer therapy. This resistance stems from the bacteria's innate ability to break down chemotherapeutic agents into inactive metabolites.[12] Infections caused by intracellular pathogenic bacteria can lead to chronic inflammation, which in turn fosters the onset and development of tumors.[13] As a consequence, timely diagnosis and effective treatment of intracellular bacterial infections are crucial for the prevention and management of both bacterial infections and their associated diseases.

In order to address these challenges, researchers have recently developed innovative solutions such as antibody-modified antibiotics, antibiotic-peptide conjugates, bacterial metabolic labeling, and other strategies.[14-19] For instance, the conjugation of an anti-*Staphylococcus aureus* antibody to an antibiotic known as rifalogue can markedly enhance the ant-bacterial potency of the antibiotic to kill intracellular bacteria.[14] Nonetheless, variations in antibody properties might compromise the effectiveness of these antibody-antibiotic conjugates, potentially limiting their broader utilization. Alternatively, probes that exploit bacterial metabolic pathways have been utilized for fluorescence labeling of intracellular bacteria residing within living host cells, as well as for in situ photodynamic eradication of bacteria.[15] Nevertheless, widespread adoption of this approach has been hindered by

its time-consuming and labor-intensive nature, along with its relatively low labeling efficiency. Furthermore, most of these approaches struggle to efficiently label and visualize intracellular bacteria, making real-time dynamic tracking of antibacterial agents' identification and killing processes against intracellular bacteria infeasible. The aforementioned situation hampers thorough investigation into the interplay between intracellular bacteria and antibacterial agents, which subsequently impedes progress in devising potent and effective antibacterial treatments. Consequently, there is an immediate need to develop advanced, biocompatible antibacterial agents that incorporate labeling and real-time imaging capabilities, allowing for specific detection and targeted elimination of intracellular bacteria.

Fluorescence imaging, characterized by its rapid response, high sensitivity, and user-friendly operation, offers unparalleled benefits in real-time, in situ visualization of molecular-level biotargets and real-time tracking of dynamic biological processes.[20,21] Nonetheless, conventional organic fluorophores, which feature expansive planar π-conjugation, tend to face significant drawbacks, such as pronounced photobleaching, suboptimal signal-to-noise ratios, and aggregation-triggered quenching (ACQ) effects.[22,23] In contrast to ACQ fluorophores, aggregation-induced emission luminogens (AIEgens) offer exceptional advantages as illuminated fluorescence imaging alternatives.[24] When AIEgens are finely distributed at the molecular level, intramolecular motions cause the dissipation of exciton energy through rapid nonradiative pathways, resulting in a nonemissive nature. However, when AIEgens aggregate, the restriction of intramolecular motions leads to strong emission, as it blocks the nonradiative decay channels.[25] Owing to their high brightness, large Stokes shifts, strong photobleaching resistance, and excellent biocompatibility, AIE-derived probes have been widely applied in the visualization of various biomolecules, complex structures, and dynamic processes, including specific biotargets analysis,[26,27] real-time subcellular or cellular imaging,[28,29] high-resolution tissue visualization,[30,31] long-term tracking of drug delivery[32,33] as well as imaging-guided disease treatment.[34,35] Furthermore, AIEgens can display additional photodynamic, photothermal, and photoacoustic properties by skillfully modulating their molecular structure. These versatile abilities have been effectively utilized in the diagnosis and therapy of pathogenic microorganisms and malignant tumors, showcasing their multifunctional potential in biomedical applications.[36,37] Traditional photosensitizers, characterized by rigid and coplanar structures, often experience reduced reactive oxygen species (ROS) sensitizing efficiency and weak fluorescence signals at high concentrations or when aggregated.[38] In contrast, AIE-active photosensitizers have been found to emit stronger fluorescence and exhibit enhanced ROS generation capabilities upon aggregation, making them well-suited for potential practical biomedical applications with their outstanding PDT properties.[39,40] However, significant challenges remain for PDT agents to achieve satisfactory therapeutic outcomes, as addressing the inherent lack of targetability in ROS and ensuring

effective delivery to the target site are critical requirements.

As a type of virus, bacteriophages demonstrate inherent specificity towards their host bacteria, enabling them to target, infiltrate, and multiply within these hosts. This ultimately results in the lysis of the host bacteria without the associated issue of antibiotic resistance.[41-43] They possess the ability to concurrently evolve and adapt to antibiotic-resistant bacterial infections.[44] Furthermore, bacteriophages, which originate from the body, exhibit excellent biocompatibility and minimal autoimmune side effects.[45] Prompted by the growing crisis in antibiotic resistance, phage therapy is experiencing a resurgence as a potent solution against bacterial infections. Numerous clinical trials are currently underway, including the use of phage cocktail therapy to combat *Acinetobacter baumannii* infections.[46] Nonetheless, conventional phage therapies often face limitations due to their modest antibacterial properties and struggles in adverse microenvironments, resulting in reduced antibacterial efficacy in real-world infections—particularly in acute cases and specific severe infectious diseases, such as those affecting immunocompromised diabetic patients.[47,48] Although it has been reported to promote the bactericidal activity of native phages by modifying with chemodynamic-active palladium nanozyme,[49] photothermal gold nanorod,[50] photocatalytic-effect quantum dot[51] and photosensitive organic dyes,[52] etc., the application of phages for intracellular bacterial labeling, imaging, and killing has not yet been reported.

Herein, we presented a novel strategy for specific imaging and killing of intracellular bacteria based on a delicately designed bacteriophage conjugate (MS2-DNA-AIEgen) commodified by aggregation-induced emission photosensitizers and DNA sequences that have intrinsic targetability to the intracellular bacteria and photodynamic inactivation (PDI) activity in bacterial killing. Serving as the foundation of the conjugate, phages maintain their innate precision targeting ability for their host bacteria. By covalently linking DNA sequences to their surfaces, phages are transformed into a classical spherical nucleic acid formula,[53,54] endowing them with the ability to penetrate infected cell membranes, navigate within cells, and ultimately target intracellular bacteria. AIEgens can label and light up the intracellular bacteria by giving a bright fluorescence signal with the guidance of phages. Subsequently, the thorough elimination of intracellular bacteria is achieved through efficient in situ ROS generation when exposed to white light, resulting in the restoration of activity in infected cells. In vitro experiments revealed that MS2-DNA-AIEgen bioconjugates exhibit one-to-one specificity and nearly 100% labeling efficiency for target bacteria, leading to a 100% mortality rate for host bacteria, while the survival rate of non-host bacteria experiences only a negligible decrease. More significantly, owing to the phage's specific targeting ability and the exceptional photodynamic efficiency of AIEgen, intracellular bacteria can be comprehensively eliminated while restoring the activity of infected and damaged macrophages. This process leads to heightened immune activity, as

evidenced by the substantial upregulation of key immune factors, such as IL-6 and TNF-α, and the downregulation of IL-10. Moreover, in bacterial-infected wound models of diabetic mice, we observed accelerated healing rates after successfully eliminating the infecting bacteria by administering MS2-DNA-AIEgen, accompanied by simultaneous positive changes in related immune factors in mice's blood, mirroring those at the cellular level. These findings demonstrate that our custom-designed multifunctional MS2-DNA-AIEgen bioconjugate combines the specific targeting abilities of bacteriophages, the potent membrane penetration of spherical nucleic acids, and the outstanding fluorescence imaging and photodynamic activity of AIE photosensitizers for coordinated imaging and extermination of intracellular bacteria. It provides a novel avenue for dealing with intracellular bacterial infection and is a good candidate for antibacterial agent screening, holding great potential for the research and theranostics of intracellular bacterial infection-related diseases in the future.

Results and Discussion

Materials Design, Preparation, and Photophysical & Bioactivity Characterization

To prepare AIE-armored bacteriophage-DNA conjugates, we initially designed and synthesized a potent AIEgen, TVP-T, featuring a positive charge and strong reactive oxygen species (ROS) generation capability. The synthesis procedure for TVP-T is thoroughly detailed in Figure S1, while its precise molecular structure is characterized using ^{1}H and ^{13}C nuclear magnetic resonance (NMR) and high-resolution mass spectroscopy (HRMS), all of which can be found in the Supporting Information.

Attributing to the existence of a positively charged pyridinium group in its structure, TVP-T could be well dissolved in a high-polarity solvent including water. More importantly, the positive charge in TVP-T endows its capability to straightforwardly attach to the negatively charged DNA sequence by electrostatic interactions. It was noteworthy that TVP-T has a strong capability of visible light absorption as its absorbance covers the range from 380 nm to 600 nm (Figure 1a). The emission could reach the near-infrared range with a maximum of 715 nm in DMSO, indicating its large Stokes shift and good potential in bioimaging with a relatively low background (Figure S2). TVP-T exhibited an apparent AIE property. No fluorescence was emitted when it was dissolved in a good solvent, DMSO, whereas strong aggregated-state emission with 54-fold enhancement in intensity appeared in 99% chloroform (Figure 1b and Figure S3). The remarkable enhancement in the absolute fluorescence quantum yield of TVP-T in chloroform (35.44%) versus in DMSO (2.77%) further verified its typical AIE feature. DNA with negative charges in phosphate-buffered saline (PBS buffer) could also induce the aggregation of TVP-T and intensify its fluorescence emission, showing a linear relationship between the emission intensity and the DNA concentration (Figures S4 and S5).

The preparation of AIE-armored bacteriophage-DNA bioconjugates was then initiated by the amino-carboxyl reaction between DNA and MS2 phage which can specifically target its host bacterium strand *Escherichia coli*-15597. As shown in Figure 1c, with the increase in the molar ratio of DNA to MS2 phage, the migration rate of the product on gel electrophoresis gradually slowed down. It no longer changed when the ratio reached 1:3000, indicating the saturation of DNA conjugations. Therefore, this ratio was chosen for the following preparation of AIE-armored bacteriophage-DNA (MS2-DNA-AIEgen) bioconjugates. As expected, TVP-T can efficiently attach to the MS2-DNA conjugates, since apparent enhancements in fluorescence intensity could be observed along with the increase of MS2-DNA concentration (Figure S5). The quantum yield of MS2-DNA-AIEgen conjugates was measured as up to 1.22%, close to the value of aggregated TVP-T in chloroform. The final molar ratio among the three components (MS2: DNA: AIEgen) in the bioconjugate was determined to be 1: 204: 1.66×10^4 after thorough ultrafiltration. Dynamic light scattering (DLS) analysis was performed to confirm the step-by-step conjugation process, with obvious increases in the average hydrodynamic diameters from 21.0 nm of original MS2 phage to 24.4 nm following DNA conjugation, and finally to 28.21 nm after TVP-T attachment (Figure S6). The gradual decrease in zeta potential further verified the successful preparation of MS2-DNA-AIEgen bioconjugates (Figure S7). The spherical morphology of the MS2 phage was kept unchanged after conjugation in TEM imaging (Figure S8). More importantly, before and after conjugation, the plaque counts of MS2 phage in elimination of its host bacteria showed negligible changes, indicating the bioconjugate has perfectly inherited the bacteriophage activity from the original MS2 (Figure 1d and Figure S9).

We next checked the photodynamic activity of the prepared bioconjugates. The strong absorption of TVP-T in the visible light region enabled us to utilize white light as the photo irradiation source. The ROS generation efficiency of the AIE photosensitizer-armored bioconjugates was initially determined by using 2′,7′-dichlorofluorescin diacetate (DCFH) as an indicator, which could emit fluorescence with a "turn-on" process triggered by ROS. As depicted in Figure 1e,f, and Figure S10, the emission intensity of DCFH gradually increased and reached 83-fold during 5 min white light irradiation (~2.0 $mW \cdot cm^{-2}$) in the presence of MS2-DNA-AIEgen bioconjugates, which was pretty higher compared to the value of 27-fold from the commercial photosensitizer, Rose Bengal, with the same concentration as the AIEgen in MS2-DNA-AIEgen bioconjugates. In contrast, DCFH alone was non-emissive and remained almost constant within the same period of exposure to white light irradiation. Additionally, compared to the~75% quantum yield of singlet oxygen ($^1O_2$) from Rose Bengal (RB) standard,[55] up to 72.5% of $^1O_2$ quantum yield for TVP-T was determined by measuring the decomposition rate of 9,10-anthracenediylbis(methylene)dimalonic acid (ABDA) as an indicator (Figure S11). Meanwhile, apparent enhancements in the emission signal could be observed from the hydroxyphenyl fluorescein (HBF) indicator for hydroxyl radicals ($OH^{\bullet}$) and the dihydrorhodamine

(DHR) indicator for superoxide radicals ($O_2^{\bullet-}$), indicating that $^1O_2$, $OH^{\bullet}$ and $O_2^{\bullet-}$ collaboratively composited the generated ROS from MS2-DNA-AIEgen bioconjugates (Figures S12 and S13). Because of these unique AIE-featured fluorescence properties and robust ROS generation capability of the prepared living bacteriophage bioconjugates in the particular recognition, imaging, and synergistic killing of pathogenic bacteria were highly expectable.

Discriminative Imaging and Killing of Bacteria in Vitro

As individual components of the MS2-DNA-AIEgen bioconjugates, the MS2 phage exhibits specific targeting of host bacteria, while the AIEgen possesses characteristic AIE properties. Together, these features ensure the high specificity and efficiency of MS2-DNA-AIEgen bioconjugates for labeling and imaging their target host bacteria, *Escherichia coli*-15597 (abbreviated as EC15597 in figures). As depicted in Figure 2a, the MS2-DNA-AIEgen bioconjugates effectively labeled *Escherichia coli*-15597, displaying a bright fluorescence signal after a 40-minute incubation period. The exceptional co-localization between the blue-colored Hoechst dye, which stains bacterial nuclei, and the red-colored AIEgen from the bioconjugates, demonstrates an almost perfect 100% staining efficiency of the MS2-DNA-AIEgen bioconjugates in targeting their host bacteria. Bacteriophage is well known for its pinpoint targetability to its host bacteria.[42,43] To assess the specificity of the MS2-DNA-AIEgen bioconjugates in targeting bacteria, MS2-host *Escherichia coli*-15597 and non-host *Escherichia coli*-8739 were co-cultured. As anticipated, the MS2-hosted *Escherichia coli*-15597 emitted a strong red fluorescence due to the binding of MS2-DNA-AIEgen bioconjugates, as shown in Figure 2b. Conversely, the non-host *Escherichia coli*-8739, characterized by a much longer morphology, remained unstained and exhibited no fluorescence. The targeting capabilities of the MS2-DNA-AIEgen bioconjugates were further investigated using a homogenous mixture consisting of MS2-host *Escherichia coli*-15597 and non-host *Escherichia coli* M15-82088. Imaging results displayed in Figure S14 revealed that the MS2-hosted *Escherichia coli*-15597 were almost entirely lit up by the MS2-DNA-AIEgen conjugates. In contrast, a negligible fluorescence signal was detected from the non-host *Escherichia coli* M15-82088, confirming that the specifically engineered MS2-DNA-AIEgen bioconjugates exhibit a high degree of specificity and labeling efficiency towards their target bacteria. When compared to the commercially available Hoechst nucleic staining, the MS2-DNA-AIEgen conjugate displayed significantly greater photostability while under continuous excitation, following its binding to the host bacteria (as shown in Figure S15). Moreover, the bioconjugate exhibited remarkable resistance to nuclease activity and maintained its structural integrity, as evidenced by negligible alterations in its photophysical properties or structural breakdown in the presence of 50 U/L DNase I or cell lysates. These findings highlight the potential of employing such bioconjugates in living cell studies (refer to Figure S16 and S17).

In addition to their distinctive fluorescence characteristics, the rapidly emerging AIE photosensitizers have proven highly effective in generating reactive oxygen species (ROS) in their aggregated state, responding to controlled external irradiation. These AIE photosensitizers have been successfully deployed in various applications, including microbial eradication, tumor suppression, and multi-faceted disease treatments.[36,56,57] Building on the demonstrated exceptional ROS generation capability of MS2-DNA-AIEgen bioconjugates, we proceeded to assess their antibacterial efficacy against both antibiotic-sensitive and drug-resistant *Escherichia coli* strains. To evaluate the combined antibacterial potential of MS2-DNA-AIEgen, MS2-host *Escherichia coli*-15597 were exposed to either bare bacteriophages (MS2), DNA-conjugated bacteriophages (MS2-DNA), or MS2-DNA-AIEgen bioconjugates for comparison. Figure S18 reveals that in the absence of light, none of these treatments effectively killed the bacteria, as bacterial survival rates consistently remained above 82%. In stark contrast, when subjected to 30 minutes of white light irradiation, MS2-DNA-AIEgen bioconjugates exhibited remarkable antibacterial action, eradicating over 99% of the host *Escherichia coli*-15597. However, under the same irradiation conditions, the MS2 phage and phage-DNA conjugate group, both containing the same phage concentration as MS2-DNA-AIEgen bioconjugates, only demonstrated 13% and 17% bactericidal efficacy, respectively. These findings underscore the critical contribution of the photodynamic activities of AIE photosensitizers within the conjugates. Similar to the results observed in the antibiotic-sensitive bacteria group, efficient inhibition of bacterial growth was also achieved in drug-resistant (DR) *Escherichia coli*-001 after treatment with 1.0×10^{10} PFU/mL of MS2-DNA-AIEgen bioconjugates (Figure 3a). As the concentration of MS2-DNA-AIEgen conjugates increased from 0 to 1.5×10^{10} PFU/mL, the bacterial survival rate of host antibiotic-sensitive *Escherichia coli*-15597 gradually decreased from 80% to 10%, demonstrating a concentration-dependent antibacterial trend (Figure 3b). This antibacterial efficiency is significantly higher than that of the bare MS2 phage, further highlighting the crucial role of the photodynamic activity of the encapsulated AIE photosensitizers in the bioconjugates (Figure S19). For the DR-type host *Escherichia coli*-001, a 100% bacterial killing efficiency was achieved by simply increasing the concentration of MS2-DNA-AIEgen bioconjugates to 5×10^{10} PFU/mL (Figure 3c). Additionally, an irradiation time-dependent bactericidal pattern was observed, as the host bacterial survival rate decreased from 100% to 2.26% when the white light irradiation time was extended from 0 minute to 30 minutes (Figure S20).

In order to investigate the specificity of MS2-DNA-AIEgen bioconjugates for targeted bacterial killing, non-host bacteria were subjected to the same treatment conditions. As evident in Figure 3a, d, no notable changes in the bacterial activity of non-host *Staphylococcus aureus*-25923 occurred across the range of tested MS2-DNA-AIEgen bioconjugate concentrations. Comparable results were

also observed in the treatment of non-host DR-type *Escherichia coli* C600-23724. As illustrated in Figure S21, the survival rate of non-host DR-type *Escherichia coli* C600-23724 remained unaffected and consistently exceeded 90%, regardless of the applied concentration of MS2-DNA-AIEgen bioconjugates. These findings demonstrate that MS2-DNA-AIEgen bioconjugates exhibit potent photodynamic inactivation (PDI) activity and intrinsic targetability to their host bacteria, resulting in the specific elimination of targeted bacteria upon light irradiation. The ensuing bacterial morphological alterations were thoroughly investigated using scanning electron microscopy (SEM) imaging. As shown in Figure 3e, f, the bacterial membranes of both antibiotic-sensitive and DR-type *Escherichia coli* exhibited significant damage upon exposure to the MS2-DNA-AIEgen bioconjugates and subsequent irradiation. A considerable number of pores and wrinkles formed on the membrane surface, leading to the distinct disintegration of the bacterial structures. In contrast, under dark conditions, the morphologies of both antibiotic-sensitive or DR-type host bacteria remained unharmed and intact. Although phage therapy itself can specifically target and inhibit the growth of host bacteria, its effectiveness is contingent upon the dosage employed. Given that a relatively low concentration of bacteriophage was used, both MS2 and MS2-DNA had only a minor impact on the treated bacteria, failing to cause widespread membrane destruction and, consequently, bacterial death (Figure S22). To further assess the antibacterial efficacy of the bacteriophage conjugates, calcein-AM and propidium iodide (PI) co-staining were employed. Notably, when treating bacteria with MS2-DNA-AIEgen bioconjugates under darkness, almost all bacteria remained alive, as evidenced by the emitted green fluorescence signal. In stark contrast, after 30 minutes of white light exposure, the mortality rates of both antibiotic-sensitive and drug-resistant bacteria approached 100%, as indicated by the red-colored PI staining (Figures S23 and S24). These findings confirm the potent antibacterial activity of the PDI-active AIEgens within these bioconjugates. To assess whether the modified phage could maintain its targetability and bactericidal activity following long-term storage, MS2-DNA-AIEgen was stored at -80°C for 7 weeks. As demonstrated in Figure S25, the host *Escherichia coli*-15597 could still be fluorescently labeled with near 100% efficiency. Furthermore, the impressive antibacterial effect was well preserved, as 1.0×10^{10} PFU/mL of MS2-DNA-AIEgen bioconjugates entirely eradicated the host bacteria upon white light exposure (Figure S26). The phage-guided targeting was crucial in achieving this exceptional antibacterial performance. Firstly, MS2 selectively identified both antibiotic-sensitive and drug-resistant (DR) *Escherichia coli* strains, binding to their membrane surfaces and initiating the phage's bacterial infection process. Subsequently, this interaction allowed the AIEgens to firmly attach themselves to the bacterial surfaces in situ, generating a significant amount of ROS upon exposure to white light. This synergy between the two processes resulted in the targeted bacteria's membrane disruption and ultimately led to their eradication.

Intracellular Bacterial Labeling, Imaging and Elimination

Macrophages that phagocytose bacteria often struggle to completely digest them, allowing the bacteria to survive and reproduce inside the phagosome. This significantly hinders the macrophages' effectiveness and can lead to severe infectious diseases.[9,10] Contrary to extracellular bacteria, those residing inside macrophages are shielded, which challenges the process of targeting and eliminating them.[11] To study the impact of intracellular bacteria on macrophages' immunity and activity, we designed an intracellular bacteria model. This involved co-incubating macrophages with MS2-hosted antibiotic-sensitive *Escherichia coli*-15597 and drug-resistant *Escherichia coli*-001 strains (see Supporting Information for details). Intracellular bacterial infections considerably impair the functionality of normal macrophages, with activity dropping from 100% to 20% as the concentration of invading bacteria increases from 0 to 4×10^7 CFU/mL (Figure S27). To assess the potential application of the designed MS2-DNA-AIEgen bioconjugates in treating bacterial-infected macrophages, the toxicities of these bioconjugates on macrophages and normal epidermal cells were first examined. As illustrated in Figure S28 and S29, regardless of illumination, the viability of RAW264.7 and HaCaT cells all remained up to 90% upon treatment by 2.4×10^{10} PFU/mL of MS2-DNA-AIEgen bioconjugates, suggesting their excellent biocompatibility. The cellular uptake efficiency of the phage conjugates was significantly enhanced due to the DNA modification surrounding the phage, as compared to those without DNA conjugation. In addition, the entry rate was accelerated (Figure S30-S32), which aligns with the widely accepted findings in the field of spherical nucleic acid systems.[53,54] After the successful endocytosis, the MS2-DNA-AIEgen bioconjugates were anticipated to locate and target the host bacteria. To achieve this, host bacteria were initially labeled with the nuclear dye, DAPI, thus creating an intracellular bacterial model. This model was established by co-incubating DAPI-stained bacteria and RAW264.7 macrophages, with the intracellular bacteria emitting blue fluorescence. As depicted in Figure 4a, following incubation with the MS2-DNA-AIEgen bioconjugates, a remarkable overlap was observed between the red fluorescence emitted by AIEgens in the bioconjugates and the blue fluorescence of intracellular bacteria, with a Pearson coefficient reaching up to 82%. The targetability of MS2-DNA-AIEgen bioconjugates towards intracellular host bacteria was further confirmed by imaging a larger area, as shown in Figure S33. To demonstrate the specificity of the MS2-DNA-AIEgen bioconjugates targeting intracellular bacteria, we established an intracellular bacterial infection model utilizing non-host *Escherichia coli*-8739. As illustrated in Figure S34, the MS2-DNA-AIEgen bioconjugates were unable to detect the non-host bacteria *Escherichia coli*-8739, failing to illuminate them with red-colored fluorescence, which aligns with the extracellular bacterial imaging outcomes. Comparable results were obtained in another intracellular bacterial model featuring non-host *Staphylococcus*

aureus-25923; there was a negligible overlap between the blue-colored bacteria and red-colored bacteriophage conjugates, with the Pearson coefficient as low as 12% (see Figure S35).

The exceptional antibacterial capabilities of MS2-DNA-AIEgen bioconjugates outside cells prompted an in-depth examination of their intracellular antibacterial performance. Infected macrophages were co-incubated with MS2-DNA-AIEgen bioconjugates and subsequently exposed to white light. Figure 4b and Figure S36 illustrate that the proportion of viable intracellular *Escherichia coli*-15597 bacteria dwindled substantially as irradiation time increased from 0 to 30 minutes—from 100% to a mere 0.52%. This decrease corresponds to the irradiation time-dependent lethal effect of MS2-DNA-AIEgen bioconjugates observed in extracellular bacteria. Next, macrophages infected with both antibiotic-sensitive and DR-type *Escherichia coli*-001 were treated using varying concentrations of MS2-DNA-AIEgen bioconjugates. As illustrated in Figure 4c and Figure S37, the remaining antibiotic-sensitive bacteria steadily decreased from 100% to 10% as the concentration of MS2-DNA-AIEgen bioconjugates increased from 0 to 2×10^{10} PFU/mL, after exposure to white light. Moreover, a stronger antibacterial effect was observed in the group of macrophages infected with DR-type *Escherichia coli*-001. A concentration of 2.4×10^{10} PFU/mL MS2-DNA-AIEgen bioconjugates was sufficient to completely eliminate the intracellular bacteria (Figure 4d and Figure S38). The activity of macrophages was observed to decrease significantly following bacterial infection, prompting further investigation into the potential of MS2-DNA-AIEgen bioconjugates to restore macrophage activity. Infected RAW264.7 cells were co-incubated with various concentrations of MS2-DNA-AIEgen conjugates for 1 hour and then exposed to white light irradiation for 30 minutes. As depicted in Figure 4e, there was a substantial increase in the activity of macrophages infected with *Escherichia coli*-15597, with activity restored from 15% to 80% after treatment with 1.6×10^{10} PFU/mL MS2-DNA-AIEgen conjugates. A similar pattern emerged for DR-type *Escherichia coli*-001 infected macrophages, as their activity levels rose from 8% to 72% following the introduction of 2.4×10^{10} PFU/mL MS2-DNA-AIEgen conjugates (Figure 4f). These findings provide compelling evidence that MS2-DNA-AIEgen conjugates are capable of specifically imaging and eradicating intracellular bacteria while simultaneously restoring the activity of infected macrophages.

To ascertain that the critical role of the photodynamic activity of AIEgen in causing the death of intracellular bacteria, we employed the DCF-DA indicator to assess and characterize the intracellular ROS generated under different treatment conditions. As demonstrated in Figures S39 and S40, macrophages treated with MS2-DNA-AIEgen conjugates exhibited a distinct bright green color upon white light irradiation, signifying the production of a substantial amount of intracellular ROS. Conversely, the fluorescence signals in the other treatment groups were considerably weaker,

suggesting that the antibacterial effect can be primarily attributed to the PDI activity of MS2-DNA-AIEgen conjugates. The morphological changes in macrophages before and after various treatments were further investigated using scanning electron microscopy (SEM) imaging. As illustrated in Figure S41a, healthy macrophages displayed three-dimensional structures with intact cell membranes and smooth surfaces. In contrast, the cell membranes of bacterially-infected macrophages exhibited noticeable damage, and endolysin from macrophages leaked out, indicating that the invasion and infection by bacteria led to the disruption and even death of macrophages (Figure S41b). Upon co-incubation with MS2-DNA-AIEgen conjugates and white light irradiation, the cellular morphology of infected macrophages showed considerable recovery, aligning with the previously established intracellular antibacterial activity. This further confirms that MS2-DNA-AIEgen conjugates can effectively restore the viability of bacterially-infected macrophages (Figure S41c).

Wound Treatment After Bacterial Infection in Diabetic Mice

Over 170 million people across the globe are affected by diabetes mellitus, and this number continues to rise. Diabetes significantly diminishes the quality of human life, leading to pain, suffering, and disability. One major complication faced by diabetic patients is impaired and delayed wound healing following bacterial infections. Wound healing is a complex process that includes interconnected and overlapping stages such as hemostasis, inflammation, proliferation, and remodeling. Macrophages are essential components in each of these phases, and they have been shown to play a pivotal role in wound tissue repair, particularly during the inflammatory stage.[58,59] We conducted a study to investigate whether MS2-DNA-AIEgen conjugates can expedite the wound healing process and prevent further wound complications in diabetic mouse models. As depicted in Figure 5a, we first created skin wounds in diabetic mice by introducing various bacteria types, including MS2-hosted antibiotic-sensitive *Escherichia coli*-15597, DR-type *Escherichia coli*-001, and non-host *Staphylococcus aureus*-25923. Once the bacterial infections were established, we applied different treatments to the wounds. We then continuously monitored the wound recovery of mice in each treatment group, collecting blood samples on day 8 to evaluate immune factors and tissue samples from the wounds on day 10 to determine the remaining bacterial count. As illustrated in the representative wound images shown in Figure 5b, it is evident that the untreated mice experienced the slowest wound healing rate, with only a 20% reduction in wound size over the course of 10 days, confirming the impaired wound healing rate in diabetic patients. Similarly, in diabetic mice treated with MS2-DNA-AIEgen conjugates under darkness, less than 50% changes in wound size occurred, as observed in the group treated with MS2-DNA and subjected to white light irradiation (Figure 5c). In stark contrast, with white light exposure, wounds infected by both antibiotic-sensitive and DR-type *Escherichia coli* exhibited over 95% recovery, and ultimately, complete healing was achieved

in 8 days. Whereas, the wound recovery rates in the group treated with MS2-DNA-AIEgen conjugates without light exposure were substantially slower, as evidenced by a less than 30% decrease in wound size. This finding highlights the essential role of AIE photosensitizers in eradicating bacteria (Figure 5d). Regardless of whether the treatment was administered in darkness or under white light irradiation, no significant changes in wound size were observed after non-host *Staphylococcus aureus*-25923 infection following treatments with MS2-DNA-AIEgen conjugate. This result confirms the remarkable specificity of the bacteriophage conjugates in addressing in vivo bacterial infections (Figure S42). After 10 days of treatment using MS2-DNA-AIEgen conjugates, it was observed that only 0.03% of MS2-hosted *Escherichia coli*-15597 and 0.46% of DR-type *Escherichia coli*-001 remained in the infected wound when exposed to white light irradiation. In contrast, for the groups treated with PBS, MS2-DNA, and MS2-DNA-AIEgen conjugates without light exposure, the corresponding bacterial counts were as high as 98% (Figure S43). These results conclusively indicate that the MS2-DNA-AIEgen conjugates exhibit enhanced antibacterial activity in vivo against both antibiotic-sensitive *Escherichia coli*-15597 and drug-resistant *Escherichia coli*-001 when exposed to white light irradiation. Furthermore, the minimal weight change observed in treated mice compared to the control group demonstrates the considerable potential for in vivo antibacterial applications of these multifunctional bacteriophage conjugates (Figure S44).

Following a 10-day treatment regimen, we collected wound tissues from the diabetic mice to further investigate the histological changes, confirming the enhanced wound healing effect provided by the MS2-DNA-AIEgen conjugates. In Figure S45, Hematoxylin-eosin (H&E) staining images reveal a notable presence of inflammatory cells in skin tissue samples treated with PBS and MS2-DNA-AIEgen conjugates in the absence of light. However, a dramatic decrease in the number of inflammatory cells is observed following treatment with MS2-DNA-AIEgen conjugates combined with white light irradiation. Additionally, the findings from TUNEL staining demonstrated that the quantity of apoptotic cells in wounds, after treatment with MS2-DNA-AIEgen conjugates combined with white light exposure, was markedly decreased in comparison to the groups treated with PBS and MS2-DNA-AIEgen conjugates without light exposure. Since collagen is a crucial component of the extracellular matrix in dermal tissue and plays a pivotal role in wound healing, the effects of the photodynamic activity of MS2-DNA-AIEgen conjugates on collagen levels in the wounded tissue were subsequently evaluated using Masson's trichrome staining. The analysis revealed significantly enhanced collagen deposition compared to the groups treated with PBS or MS2-DNA-AIEgen conjugates under dark conditions. Moreover, CD31 expression in the group treated with MS2-DNA-AIEgen conjugates and exposed to irradiation was notably higher compared to the PBS and MS2-DNA-AIEgen conjugates groups without light exposure. Wound tissue cell proliferation was further evaluated using Ki67 staining. Similar to the PBS control group, there were no significant changes in

Ki67 expression levels in the group treated with MS2-DNA-AIEgen conjugates without light exposure. In contrast, a substantially reduced expression level was observed when light irradiation was applied. As the wound healed, it transitioned from the proliferative stage to the remodeling stage, which accounts for the decrease in Ki67 expression levels following treatment with MS2-DNA-AIEgen conjugates and white light irradiation.

The peptidoglycan, lipopolysaccharide, flagellum, and other distinct bacterial components can be detected by the pattern recognition receptors present on macrophages and other immune cells, thereby triggering an immune response.[60] Bacterial infection significantly impairs the activity of macrophages, leading to reduced or even lost immunogenicity. By employing photodynamic therapy with MS2-DNA-AIEgen conjugates, bacteria internalized within macrophages can be effectively eliminated. Following the breakdown of dead bacteria carrying lipopolysaccharide, it is likely that macrophage immune responses will be activated, leading to the production of immunologically active substances.[61] As demonstrated in Figure 6a-c, ELISA tests revealed that the expression levels of both IL-6 and TNF-α surged by over 500% after treating macrophages with MS2-DNA-AIEgen conjugates and white light irradiation. In contrast, IL-10 levels exhibited a significant decline, reflecting a substantial activation of macrophage immunity. In vivo samples collected from the blood of diabetic mice after various treatments were analyzed for the presence of immune-active substances. Consistent with the previous findings, mice infected with MS2-host antibiotic-sensitive and drug-resistant strains of *Escherichia coli* exhibited increased levels of IL-6 and TNF-α, and significantly reduced levels of IL-10 after treatment with MS2-DNA-AIEgen conjugates and exposure to white light (Figure 6d-f). These findings further confirm the activation of immunological effects. Our results demonstrate that MS2-DNA-AIEgen conjugates not only restore macrophage activity but also stimulate an immune response in these cells, indicating a strong potential for effective long-term bactericidal action both intracellularly and in vivo.

Conclusion

In summary, we have ingeniously developed an innovative multifunctional phage bioconjugate system (MS2-DNA-AIEgen) specifically tailored to address intracellular bacterial infections. This sophisticated bioconjugate is carefully crafted by incorporating AIE photosensitizers and nucleic acid sequences onto the bacteriophage surface. The integration of nucleic acids transforms the bacteriophage into a prototypical spherical nucleic acid, which significantly enhances the conjugate's ability to penetrate mammalian cell membrane barriers. Subsequently, this allows for precise targeting and labeling of the intracellular bacteria. Furthermore, the AIE photosensitizer boasts distinctive fluorescence characteristics and potent photodynamic activity, facilitating the vivid fluorescence imaging of intracellular bacteria. Thanks to the ROS generation capability of the MS2-

DNA-AIEgen bioconjugates under external white light irradiation, the complete elimination of intracellular bacteria was achieved, simultaneously restoring the viability of the infected macrophages. In vitro studies have demonstrated that MS2-DNA-AIEgen bioconjugates exhibit exceptional specificity in identifying target bacteria, successfully eliminating 100% of both antibiotic-sensitive and drug-resistant host strains without affecting non-host bacteria, which maintain a 100% survival rate. Furthermore, intracellular investigations have confirmed that these bioconjugates can effectively target and eradicate infected bacteria within macrophages while maintaining excellent biocompatibility. Remarkable antibacterial activity was observed, along with accelerated healing of bacterial-infected wounds in diabetic mice, without any impact on their growth. Furthermore, the MS2-DNA-AIEgen bioconjugates show potential to induce immune responses in infected macrophage cells and diabetic mice, suggesting their potential for long-term antibacterial applications. Our research introduces a groundbreaking approach to combating severe intracellular bacterial infections, exhibiting significant promise for the identification of novel therapeutic agents targeting intracellular bacterial infection, as well as advancing the theranostics of associated malignancies resulting from such infections.

Notes

The authors declare no competing financial interest.

ACKNOWLEDGMENTS

The authors acknowledge funding from the National Science Foundation of China (22274106, 22104104), the Natural Science Foundation of Jiangsu Province (BK20210701), the Program of Suzhou Innovation and Entrepreneurship Leading Talents (ZXL2022513) and startup funds from Soochow University.

REFERENCES

(1) Brown, E. D.; Wright, G. D. Antibacterial Drug Discovery in the Resistance Era. *Nature* **2016,** *529*, 336-343.

(2) Kupferschmidt, K. Resistance Fighters. *Science* **2016,** *352*, 758-761.

(3) Murray, C. J. L.; Ikuta, K. S.; Sharara, F.; Swetschinski, L.; Robles Aguilar, G.; Gray, A.; Han, C.; Bisignano, C.; Rao, P.; Wool, E.; Johnson, S. C.; Browne, A. J.; Chipeta, M. G.; Fell, F.; Hackett, S.; Haines-Woodhouse, G.; Kashef Hamadani, B. H.; Kumaran, E. A. P.; McManigal, B.; Achalapong, S.; Agarwal, R.; Akech, S.; Albertson, S.; Amuasi, J.; Andrews, J.; Aravkin, A.; Ashley, E.; Babin, F.-X.; Bailey, F.; Baker, S.; Basnyat, B.; Bekker, A.; Bender, R.; Berkley, J. A.; Bethou, A.; Bielicki, J.; Boonkasidecha, S.; Bukosia, J.; Carvalheiro, C.; Castañeda-Orjuela, C.; Chansamouth, V.; Chaurasia, S.; Chiurchiù, S.; Chowdhury, F.; Clotaire Donatien, R.; Cook, A. J.; Cooper, B.; Cressey, T. R.; Criollo-Mora, E.; Cunningham, M.; Darboe, S.; Day, N. P. J.; De Luca, M.; Dokova, K.; Dramowski, A.; Dunachie, S. J.; Duong Bich, T.; Eckmanns, T.; Eibach, D.; Emami, A.; Feasey, N.; Fisher-Pearson, N.; Forrest, K.; Garcia, C.; Garrett, D.; Gastmeier, P.; Giref, A. Z.; Greer, R. C.; Gupta, V.; Haller, S.; Haselbeck, A.; Hay, S. I.; Holm, M.; Hopkins, S.; Hsia, Y.; Iregbu, K. C.; Jacobs, J.; Jarovsky, D.; Javanmardi, F.; Jenney, A. W. J.; Khorana, M.; Khusuwan, S.; Kissoon, N.; Kobeissi,

E.; Kostyanev, T.; Krapp, F.; Krumkamp, R.; Kumar, A.; Kyu, H. H.; Lim, C.; Lim, K.; Limmathurotsakul, D.; Loftus, M. J.; Lunn, M.; Ma, J.; Manoharan, A.; Marks, F.; May, J.; Mayxay, M.; Mturi, N. Global Burden of Bacterial Antimicrobial Resistance in 2019: A Systematic Analysis. *The Lancet* **2022,** *399*, 629-655.
(4) Martirosyan, A.; Moreno, E.; Gorvel, J.-P. An Evolutionary Strategy for a Stealthy Intracellular Brucella Pathogen. *Immunol. Rev.* **2011,** *240*, 211-234.
(5) Finlay, B. B.; Cossart, P. Exploitation of Mammalian Host Cell Functions by Bacterial Pathogens. *Science* **1997,** *276*, 718-725.
(6) Sandberg, A.; Hessler, J. H. R.; Skov, R. L.; Blom, J.; Frimodt-Møller, N. Intracellular Activity of Antibiotics against Staphylococcus Aureus in a Mouse Peritonitis Model. *Antimicrob. Agents Ch.* **2009,** *53*, 1874-1883.
(7) DuMont, A. L.; Yoong, P.; Surewaard, B. G. J.; Benson, M. A.; Nijland, R.; Strijp, J. A. G. v.; Torres, V. J. Staphylococcus Aureus Elaborates Leukocidin Ab to Mediate Escape from within Human Neutrophils. *Infect. Immun.* **2013,** *81*, 1830-1841.
(8) Guo, H.; Callaway, J. B.; Ting, J. P. Y. Inflammasomes: Mechanism of Action, Role in Disease, and Therapeutics. *Nat. Med.* **2015,** *21*, 677-687.
(9) Bussi, C.; Gutierrez, M. G. Mycobacterium Tuberculosis Infection of Host Cells in Space and Time. *FEMS Microbiol. Rev.* **2019,** *43*, 341-361.
(10) Mellouk, N.; Enninga, J. Cytosolic Access of Intracellular Bacterial Pathogens: The Shigella Paradigm. *Front. Cell. Infect. Microbiol.* **2016,** *6*, 35.
(11) Kamaruzzaman, N. F.; Kendall, S.; Good, L. Targeting the Hard to Reach: Challenges and Novel Strategies in the Treatment of Intracellular Bacterial Infections. *Brit. J. Pharmacol.* **2017,** *174*, 2225-2236.
(12) Geller, L. T.; Barzily-Rokni, M.; Danino, T.; Jonas, O. H.; Shental, N.; Nejman, D.; Gavert, N.; Zwang, Y.; Cooper, Z. A.; Shee, K.; Thaiss, C. A.; Reuben, A.; Livny, J.; Avraham, R.; Frederick, D. T.; Ligorio, M.; Chatman, K.; Johnston, S. E.; Mosher, C. M.; Brandis, A.; Fuks, G.; Gurbatri, C.; Gopalakrishnan, V.; Kim, M.; Hurd, M. W.; Katz, M.; Fleming, J.; Maitra, A.; Smith, D. A.; Skalak, M.; Bu, J.; Michaud, M.; Trauger, S. A.; Barshack, I.; Golan, T.; Sandbank, J.; Flaherty, K. T.; Mandinova, A.; Garrett, W. S.; Thayer, S. P.; Ferrone, C. R.; Huttenhower, C.; Bhatia, S. N.; Gevers, D.; Wargo, J. A.; Golub, T. R.; Straussman, R. Potential Role of Intratumor Bacteria in Mediating Tumor Resistance to the Chemotherapeutic Drug Gemcitabine. *Science* **2017,** *357*, 1156-1160.
(13) Armstrong, H.; Bording-Jorgensen, M.; Dijk, S.; Wine, E. The Complex Interplay between Chronic Inflammation, the Microbiome, and Cancer: Understanding Disease Progression and What We Can Do to Prevent It. *Cancers* **2018,** *10*, 83.
(14) Lehar, S. M.; Pillow, T.; Xu, M.; Staben, L.; Kajihara, K. K.; Vandlen, R.; DePalatis, L.; Raab, H.; Hazenbos, W. L.; Hiroshi Morisaki, J.; Kim, J.; Park, S.; Darwish, M.; Lee, B.-C.; Hernandez, H.; Loyet, K. M.; Lupardus, P.; Fong, R.; Yan, D.; Chalouni, C.; Luis, E.; Khalfin, Y.; Plise, E.; Cheong, J.; Lyssikatos, J. P.; Strandh, M.; Koefoed, K.; Andersen, P. S.; Flygare, J. A.; Wah Tan, M.; Brown, E. J.; Mariathasan, S. Novel Antibody–Antibiotic Conjugate Eliminates Intracellular S. Aureus. *Nature* **2015,** *527*, 323-328.
(15) Hu, F.; Qi, G.; Kenry; Mao, D.; Zhou, S.; Wu, M.; Wu, W.; Liu, B. Visualization and in Situ Ablation of Intracellular Bacterial Pathogens through Metabolic Labeling. *Angew. Chem. Int. Ed.* **2020,** *59*, 9288-9292.
(16) Zhan, W.; Xu, L.; Liu, Z.; Liu, X.; Gao, G.; Xia, T.; Cheng, X.; Sun, X.; Wu, F.-G.; Yu, Q.; Liang,

G. Tandem Guest-Host-Receptor Recognitions Precisely Guide Ciprofloxacin to Eliminate Intracellular Staphylococcus Aureus. *Angew. Chem. Int. Ed.* **2023,** *62*, e202306427.
(17) Pereira, M. P.; Shi, J.; Kelley, S. O. Peptide Targeting of an Antibiotic Prodrug toward Phagosome-Entrapped Mycobacteria. *ACS Infect. Dis.* **2015,** *1*, 586-592.
(18) Brezden, A.; Mohamed, M. F.; Nepal, M.; Harwood, J. S.; Kuriakose, J.; Seleem, M. N.; Chmielewski, J. Dual Targeting of Intracellular Pathogenic Bacteria with a Cleavable Conjugate of Kanamycin and an Antibacterial Cell-Penetrating Peptide. *J. Am. Chem. Soc.* **2016,** *138*, 10945-10949.
(19) Qi, G.-B.; Zhang, D.; Liu, F.-H.; Qiao, Z.-Y.; Wang, H. An "On-Site Transformation" Strategy for Treatment of Bacterial Infection. *Adv. Mater.* **2017,** *29*, 1703461.
(20) Kobayashi, H.; Ogawa, M.; Alford, R.; Choyke, P. L.; Urano, Y. New Strategies for Fluorescent Probe Design in Medical Diagnostic Imaging. *Chem. Rev.* **2010,** *110*, 2620-2640.
(21) Baker, M. The Whole Picture. *Nature* **2010,** *463*, 977-979.
(22) Mei, J.; Leung, N. L. C.; Kwok, R. T. K.; Lam, J. W. Y.; Tang, B. Z. Aggregation-Induced Emission: Together We Shine, United We Soar! *Chem. Rev.* **2015,** *115*, 11718-11940.
(23) Birks, J. B. Photophysics of Aromatic Molecules. *Wiley: London* **1970**.
(24) Kwok, R. T. K.; Leung, C. W. T.; Lam, J. W. Y.; Tang, B. Z. Biosensing by Luminogens with Aggregation-Induced Emission Characteristics. *Chem. Soc. Rev.* **2015,** *44*, 4228-4238.
(25) Leung, N. L. C.; Xie, N.; Yuan, W.; Liu, Y.; Wu, Q.; Peng, Q.; Miao, Q.; Lam, J. W. Y.; Tang, B. Z. Restriction of Intramolecular Motions: The General Mechanism Behind Aggregation-Induced Emission. *Chem–Eur. J.* **2014,** *20*, 15349-15353.
(26) Gao, Y.; He, Z.; He, X.; Zhang, H.; Weng, J.; Yang, X.; Meng, F.; Luo, L.; Tang, B. Z. Dual-Color Emissive AIEgen for Specific and Label-Free Double-Stranded DNA Recognition and Single-Nucleotide Polymorphisms Detection. *J. Am. Chem. Soc.* **2019,** *141*, 20097-20106.
(27) Xiong, L.-H.; He, X.; Zhao, Z.; Kwok, R. T. K.; Xiong, Y.; Gao, P. F.; Yang, F.; Huang, Y.; Sung, H. H. Y.; Williams, I. D.; Lam, J. W. Y.; Cheng, J.; Zhang, R.; Tang, B. Z. Ultrasensitive Virion Immunoassay Platform with Dual-Modality Based on a Multifunctional Aggregation-Induced Emission Luminogen. *ACS Nano* **2018,** *12*, 9549-9557.
(28) He, X.; Zhao, Z.; Xiong, L.-H.; Gao, P. F.; Peng, C.; Li, R. S.; Xiong, Y.; Li, Z.; Sung, H. H. Y.; Williams, I. D.; Kwok, R. T. K.; Lam, J. W. Y.; Huang, C. Z.; Ma, N.; Tang, B. Z. Redox-Active AIEgen-Derived Plasmonic and Fluorescent Core@Shell Nanoparticles for Multimodality Bioimaging. *J. Am. Chem. Soc.* **2018,** *140*, 6904-6911.
(29) Niu, G.; Zheng, X.; Zhao, Z.; Zhang, H.; Wang, J.; He, X.; Chen, Y.; Shi, X.; Ma, C.; Kwok, R. T. K.; Lam, J. W. Y.; Sung, H. H. Y.; Williams, I. D.; Wong, K. S.; Wang, P.; Tang, B. Z. Functionalized Acrylonitriles with Aggregation-Induced Emission: Structure Tuning by Simple Reaction-Condition Variation, Efficient Red Emission, and Two-Photon Bioimaging. *J. Am. Chem. Soc.* **2019,** *141*, 15111-15120.
(30) Wang, S.; Liu, J.; Goh, C. C.; Ng, L. G.; Liu, B. NIR- II -Excited Intravital Two-Photon Microscopy Distinguishes Deep Cerebral and Tumor Vasculatures with an Ultrabright NIR- I AIE Luminogen. *Adv. Mater.* **2019,** *31*, 1904447.
(31) Sheng, Z.; Guo, B.; Hu, D.; Xu, S.; Wu, W.; Liew, W. H.; Yao, K.; Jiang, J.; Liu, C.; Zheng, H.; Liu, B. Bright Aggregation-Induced-Emission Dots for Targeted Synergetic NIR- II Fluorescence and NIR- I Photoacoustic Imaging of Orthotopic Brain Tumors. *Adv. Mater.* **2018,** *30*, 1800766.

(32) Sun, J.; He, X. AIE-Based Drug/Gene Delivery System: Evolution from Fluorescence Monitoring Alone to Augmented Therapeutics. *Aggregate* **2022,** *3*, e282.
(33) Wang, Y.; Zhang, Y.; Wang, J.; Liang, X.-J. Aggregation-Induced Emission (AIE) Fluorophores as Imaging Tools to Trace the Biological Fate of Nano-Based Drug Delivery Systems. *Adv. Drug Deliver. Rev.* **2019,** *143*, 161-176.
(34) Wang, C.; Fan, W.; Zhang, Z.; Wen, Y.; Xiong, L.; Chen, X. Advanced Nanotechnology Leading the Way to Multimodal Imaging-Guided Precision Surgical Therapy. *Adv. Mater.* **2019,** *31*, 1904329.
(35) Li, Y.; Fan, X.; Li, Y.; Zhu, L.; Chen, R.; Zhang, Y.; Ni, H.; Xia, Q.; Feng, Z.; Tang, B. Z.; Qian, J.; Lin, H. Biologically Excretable AIE Nanoparticles Wear Tumor Cell-Derived "Exosome Caps" for Efficient NIR- II Fluorescence Imaging-Guided Photothermal Therapy. *Nano Today* **2021,** *41*, 101333.
(36) Hu, F.; Xu, S.; Liu, B. Photosensitizers with Aggregation-Induced Emission: Materials and Biomedical Applications. *Adv. Mater.* **2018,** *30*, 1801350.
(37) Qian, J.; Tang, B. Z. AIE Luminogens for Bioimaging and Theranostics: From Organelles to Animals. *Chem* **2017,** *3*, 56-91.
(38) Feng, G.; Zhang, G.-Q.; Ding, D. Design of Superior Phototheranostic Agents Guided by Jablonski Diagrams. *Chem. Soc. Rev.* **2020,** *49*, 8179-8234.
(39) Liu, Z.; Zhang, J.; Liu, H.; Shen, H.; Meng, N.; Qi, X.; Ding, K.; Song, J.; Fu, R.; Ding, D.; Feng, G. BSA-AIE Nanoparticles with Boosted Ros Generation for Immunogenic Cell Death Immunotherapy of Multiple Myeloma. *Adv. Mater.* **2023,** *35*, 2208692.
(40) Zhang, Z.; Kang, M.; Tan, H.; Song, N.; Li, M.; Xiao, P.; Yan, D.; Zhang, L.; Wang, D.; Tang, B. Z. The Fast-Growing Field of Photo-Driven Theranostics Based on Aggregation-Induced Emission. *Chem. Soc. Rev.* **2022,** *51*, 1983-2030.
(41) Kalelkar, P. P.; Riddick, M.; García, A. J. Biomaterial-Based Antimicrobial Therapies for the Treatment of Bacterial Infections. *Nat. Rev. Mater.* **2022,** *7*, 39-54.
(42) Kutateladze, M.; Adamia, R. Bacteriophages as Potential New Therapeutics to Replace or Supplement Antibiotics. *Trends Biotechnol.* **2010,** *28*, 591-595.
(43) Nobrega, F. L.; Vlot, M.; de Jonge, P. A.; Dreesens, L. L.; Beaumont, H. J. E.; Lavigne, R.; Dutilh, B. E.; Brouns, S. J. J. Targeting Mechanisms of Tailed Bacteriophages. *Nat. Rev. Microbiol.* **2018,** *16*, 760-773.
(44) Thiel, K. Old Dogma, New Tricks—21st Century Phage Therapy. *Nat. Biotechnol.* **2004,** *22*, 31-36.
(45) Cao, B.; Li, Y.; Yang, T.; Bao, Q.; Yang, M.; Mao, C. Bacteriophage-Based Biomaterials for Tissue Regeneration. *Adv. Drug Deliver. Rev.* **2019,** *145*, 73-95.
(46) Hatfull, G. F.; Dedrick, R. M.; Schooley, R. T. Phage Therapy for Antibiotic-Resistant Bacterial Infections. *Annu. Rev. Med.* **2022,** *73*, 197-211.
(47) Hampton, H. G.; Watson, B. N. J.; Fineran, P. C. The Arms Race between Bacteria and Their Phage Foes. *Nature* **2020,** *577*, 327-336.
(48) Schooley, R. T.; Biswas, B.; Gill, J. J.; Hernandez-Morales, A.; Lancaster, J.; Lessor, L.; Barr, J. J.; Reed, S. L.; Rohwer, F.; Benler, S.; Segall, A. M.; Taplitz, R.; Smith, D. M.; Kerr, K.; Kumaraswamy, M.; Nizet, V.; Lin, L.; McCauley, M. D.; Strathdee, S. A.; Benson, C. A.; Pope, R. K.; Leroux, B. M.; Picel, A. C.; Mateczun, A. J.; Cilwa, K. E.; Regeimbal, J. M.; Estrella, L. A.; Wolfe, D. M.; Henry, M. S.; Quinones, J.; Salka, S.; Bishop-Lilly, K. A.; Young, R.; Hamilton, T. Development and Use of

Personalized Bacteriophage-Based Therapeutic Cocktails to Treat a Patient with a Disseminated Resistant Acinetobacter Baumannii Infection. *Antimicrob. Agents Ch.* **2017,** *61*, 10.1128/aac.00954-00917.
(49) Jin, L.; Cao, F.; Gao, Y.; Zhang, C.; Qian, Z.; Zhang, J.; Mao, Z. Microenvironment-Activated Nanozyme-Armed Bacteriophages Efficiently Combat Bacterial Infection. *Adv. Mater.* **2023,** *35*, 2301349.
(50) Peng, H.; Borg, R. E.; Dow, L. P.; Pruitt, B. L.; Chen, I. A. Controlled Phage Therapy by Photothermal Ablation of Specific Bacterial Species Using Gold Nanorods Targeted by Chimeric Phages. *Proc. Natl. Acad. Sci. U.S.A.* **2020,** *117*, 1951-1961.
(51) Wang, L.; Fan, X.; Gonzalez Moreno, M.; Tkhilaishvili, T.; Du, W.; Zhang, X.; Nie, C.; Trampuz, A.; Haag, R. Photocatalytic Quantum Dot-Armed Bacteriophage for Combating Drug-Resistant Bacterial Infection. *Adv. Sci.* **2022,** *9*, 2105668.
(52) He, X.; Yang, Y.; Guo, Y.; Lu, S.; Du, Y.; Li, J.-J.; Zhang, X.; Leung, N. L. C.; Zhao, Z.; Niu, G.; Yang, S.; Weng, Z.; Kwok, R. T. K.; Lam, J. W. Y.; Xie, G.; Tang, B. Z. Phage-Guided Targeting, Discriminative Imaging, and Synergistic Killing of Bacteria by AIE Bioconjugates. *J. Am. Chem. Soc.* **2020,** *142*, 3959-3969.
(53) Cutler, J. I.; Auyeung, E.; Mirkin, C. A. Spherical Nucleic Acids. *J. Am. Chem. Soc.* **2012,** *134*, 1376-1391.
(54) Li, H.; Zhang, B.; Lu, X.; Tan, X.; Jia, F.; Xiao, Y.; Cheng, Z.; Li, Y.; Silva, D. O.; Schrekker, H. S.; Zhang, K.; Mirkin, C. A. Molecular Spherical Nucleic Acids. *Proc. Natl. Acad. Sci. U.S.A.* **2018,** *115*, 4340-4344.
(55) Lambert, C. R.; Kochevar, I. E. Does Rose Bengal Triplet Generate Superoxide Anion? *J. Am. Chem. Soc.* **1996,** *118*, 3297-3298.
(56) He, X.; Xiong, L.-H.; Zhao, Z.; Wang, Z.; Luo, L.; Lam, J. W. Y.; Kwok, R. T. K.; Tang, B. Z. AIE-Based Theranostic Systems for Detection and Killing of Pathogens. *Theranostics* **2019,** *9*, 3223.
(57) Wang, H.; Li, Q.; Alam, P.; Bai, H.; Bhalla, V.; Bryce, M. R.; Cao, M.; Chen, C.; Chen, S.; Chen, X.; Chen, Y.; Chen, Z.; Dang, D.; Ding, D.; Ding, S.; Duo, Y.; Gao, M.; He, W.; He, X.; Hong, X.; Hong, Y.; Hu, J.-J.; Hu, R.; Huang, X.; James, T. D.; Jiang, X.; Konishi, G.-i.; Kwok, R. T. K.; Lam, J. W. Y.; Li, C.; Li, H.; Li, K.; Li, N.; Li, W.-J.; Li, Y.; Liang, X.-J.; Liang, Y.; Liu, B.; Liu, G.; Liu, X.; Lou, X.; Lou, X.-Y.; Luo, L.; McGonigal, P. R.; Mao, Z.-W.; Niu, G.; Owyong, T. C.; Pucci, A.; Qian, J.; Qin, A.; Qiu, Z.; Rogach, A. L.; Situ, B.; Tanaka, K.; Tang, Y.; Wang, B.; Wang, D.; Wang, J.; Wang, W.; Wang, W.-X.; Wang, W.-J.; Wang, X.; Wang, Y.-F.; Wu, S.; Wu, Y.; Xiong, Y.; Xu, R.; Yan, C.; Yan, S.; Yang, H.-B.; Yang, L.-L.; Yang, M.; Yang, Y.-W.; Yoon, J.; Zang, S.-Q.; Zhang, J.; Zhang, P.; Zhang, T.; Zhang, X.; Zhang, X.; Zhao, N.; Zhao, Z.; Zheng, J.; Zheng, L.; Zheng, Z.; Zhu, M.-Q.; Zhu, W.-H.; Zou, H.; Tang, B. Z. Aggregation-Induced Emission (AIE), Life and Health. *ACS Nano* **2023,** *17*, 14347-14405.
(58) Liu, D.; Yang, P.; Gao, M.; Yu, T.; Shi, Y.; Zhang, M.; Yao, M.; Liu, Y.; Zhang, X. NLRP3 Activation Induced by Neutrophil Extracellular Traps Sustains Inflammatory Response in the Diabetic Wound. *Clin. Sci.* **2019,** *133*, 565-582.
(59) Lucas, T.; Waisman, A.; Ranjan, R.; Roes, J.; Krieg, T.; Müller, W.; Roers, A.; Eming, S. A. Differential Roles of Macrophages in Diverse Phases of Skin Repair. *J. Immunol.* **2010,** *184*, 3964-3977.
(60) Zitvogel, L.; Ayyoub, M.; Routy, B.; Kroemer, G. Microbiome and Anticancer Immunosurveillance. *Cell* **2016,** *165*, 276-287.

(61) Triantafilou, M.; Triantafilou, K. Lipopolysaccharide Recognition: CD14, TLRs and the LPS-Activation Cluster. *Trends Immunol.* **2002,** *23*, 301-304.

Scheme 1. Schematic illustration of the delicately designed bacteriophage bioconjugate (MS2-DNA-AIEgen) for specific targeting and synergistic elimination of intracellular bacteria[a]

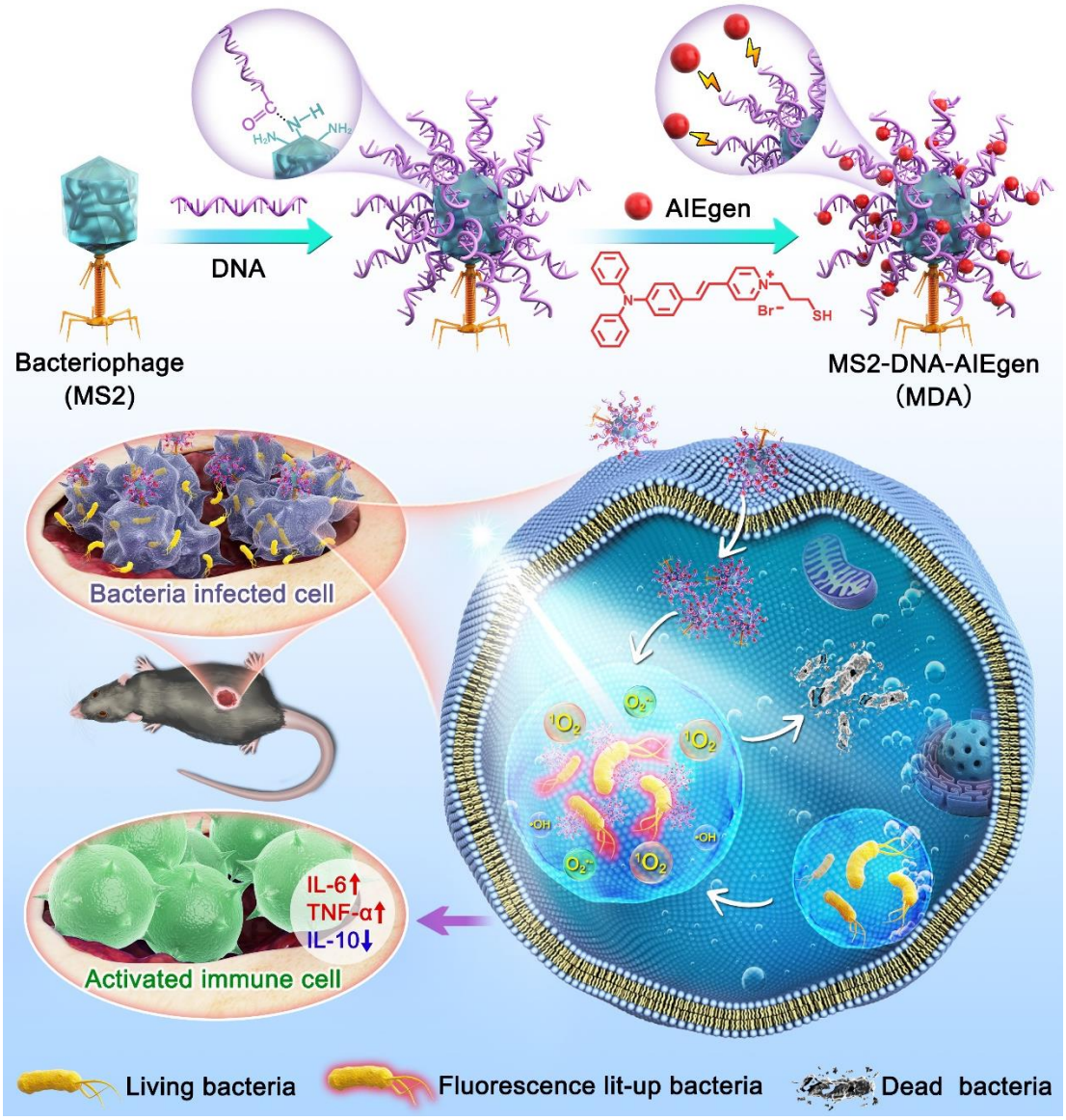

[a]In the preparation of bacteriophage bioconjugate, DNA was covalently linked to the surface of the bacteriophage via an amino-carboxyl coupling reaction. The positively charged AIEgens were then bound to the DNA via electrostatic interaction. Taking advantage of the surface anchoring of DNA, the formed bacteriophage bioconjugates resemble spheric nucleic acid and are capable of entering the mammalian cell (e.g. RAW264.7 macrophages) and targeting the intracellular bacteria under the guidance of bacteriophage. Upon white light irradiation, the robust AIE-active photosensitizers can efficiently generate ROS species, affording synergistic antibacterial outcomes along with the intricate antibacterial capability of bacteriophage towards its host bacteria, as well as the enhanced immune response at the cell and body level.

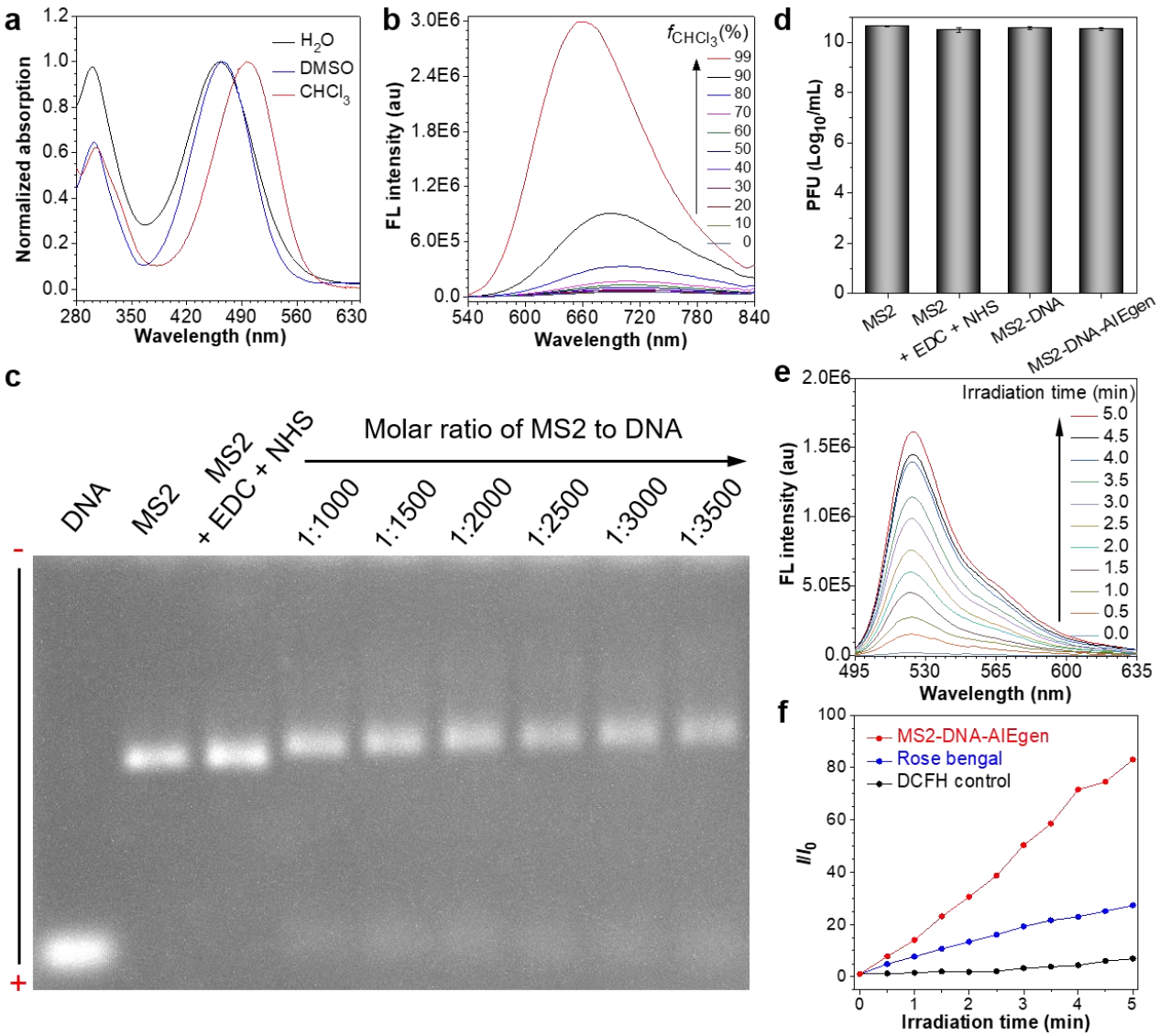

Figure 1. (a) Normalized UV−vis spectra of AIEgen (TVP-T) dissolved in water, DMSO, and $CHCl_3$, respectively. (b) AIE curve of TVP-T in the mixture of DMSO and $CHCl_3$ with varying volume fractions of $CHCl_3$. (c) Agarose gel electrophoresis for monitoring the conjugation between bacteriophage and DNA with various molar ratios. The DNA was modified with FAM dye. (d) Activity test of bacteriophage before and after conjugation reactions. (e) Chemical trapping of the total ROS generation efficiency of MS2-DNA-AIEgen bioconjugates indicated by the photoactivation of DCFH indicator. (f) Activation rates of the DCFH indicator reacted with various chemical agents that were monitored at the emission maximum of 524 nm. These measurements were carried out under white light irradiation in 1× PBS buffer. [AIEgen in MS2-DNA-AIEgen conjugate] = [Rose Bengal] = 1.0 μM, [DCFH]= 10 μM.

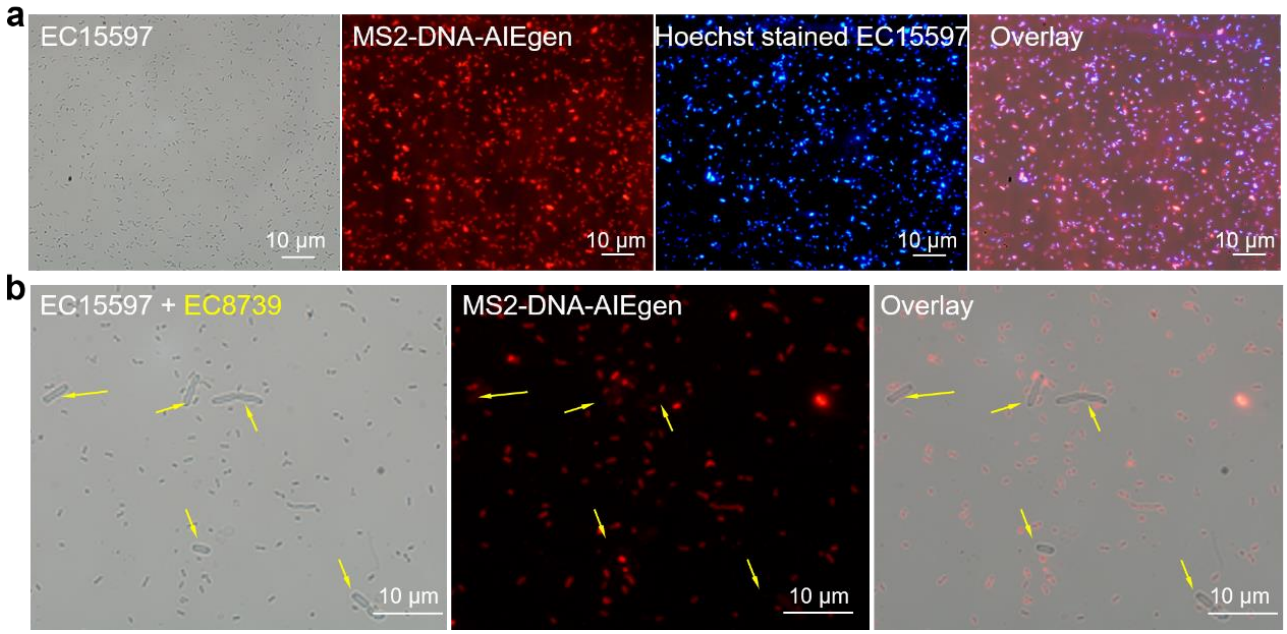

Figure 2. Targeted bacterial labeling and imaging by MS2-DNA-AIEgen bioconjugates. (a) Fluorescence imaging of MS2-hosted *Escherichia coli*-15597 coincubated with MS2-DNA-AIEgen for 40 min. (b) Specificity test of MS2-DNA-AIEgen towards its host bacteria by coincubation of host *Escherichia coli*-15597 and non-host *Escherichia coli*-8739. Arrows indicated the non-host *Escherichia coli*-8739 that was not stained by the red-color emissive MS2-DNA-AIEgen.

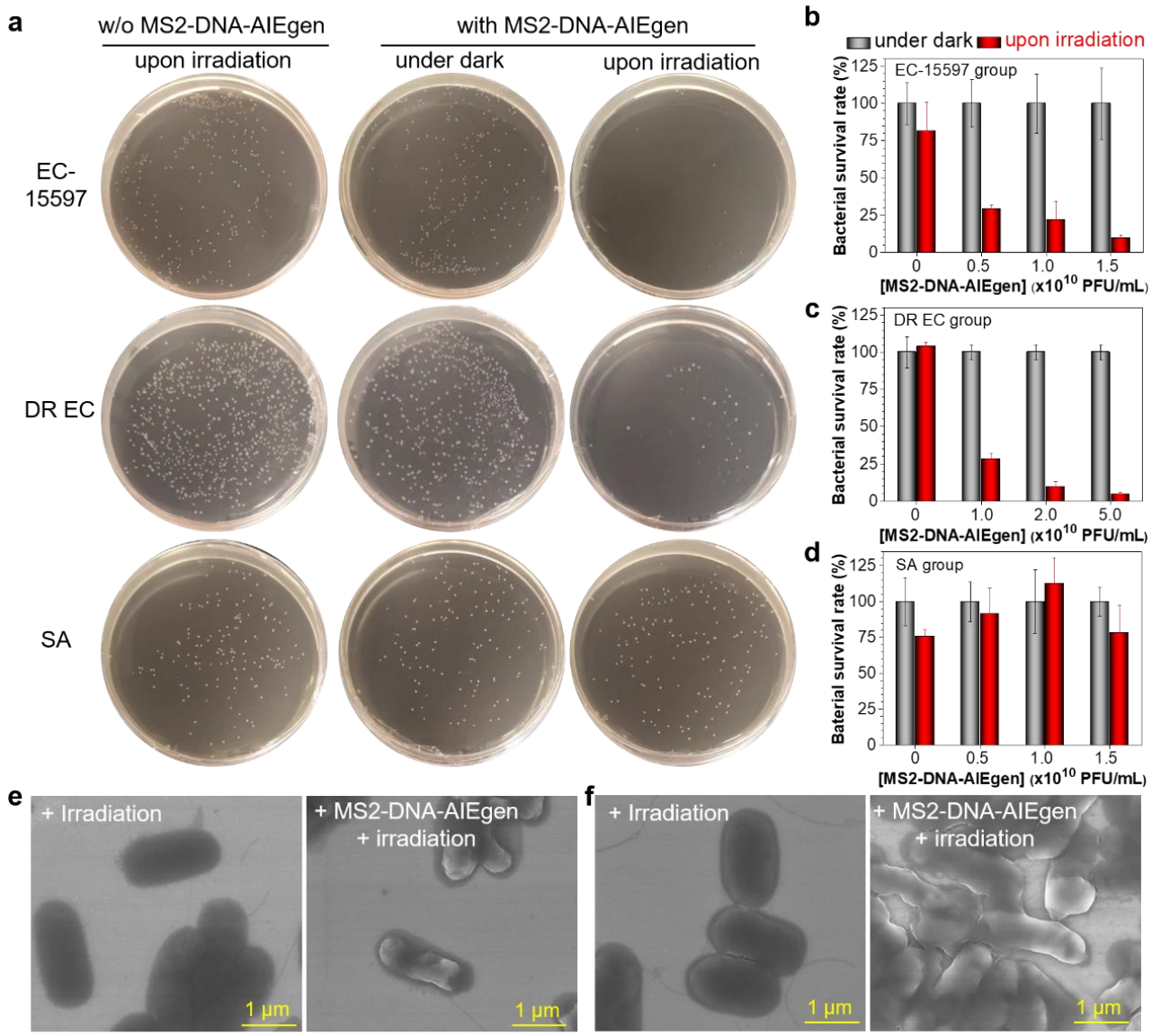

Figure 3. Antibacterial evaluation of MS2-DNA-AIEgen bioconjugates. (a) The plaque counts of host *Escherichia coli*-15597 (2.0×10^6 CFU·mL^{-1}), DR-type host *Escherichia coli*-001 (1.0×10^6 CFU·mL^{-1}), and non-host S*taphylococcus aureus*-25923 (2.0×10^6 CFU·mL^{-1}) under various treatments. (b) The calculated survival rate of host *Escherichia coli*-15597 along with varying concentrations of MS2-DNA-AIEgen under dark or white light irradiation, respectively. (c) The calculated survival rate of DR-type host *Escherichia coli*-001 along with varying concentrations of MS2-DNA-AIEgen, under dark or white light irradiation, respectively. (d) The calculated survival rate of non-host S*taphylococcus aureus*-25923 along with varying concentrations of MS2-DNA-AIEgen, under dark or white light irradiation, respectively. (e) and (f) SEM images of the morphologies of treated host *Escherichia coli*-15597 and DR-type host *Escherichia coli*-001, respectively.

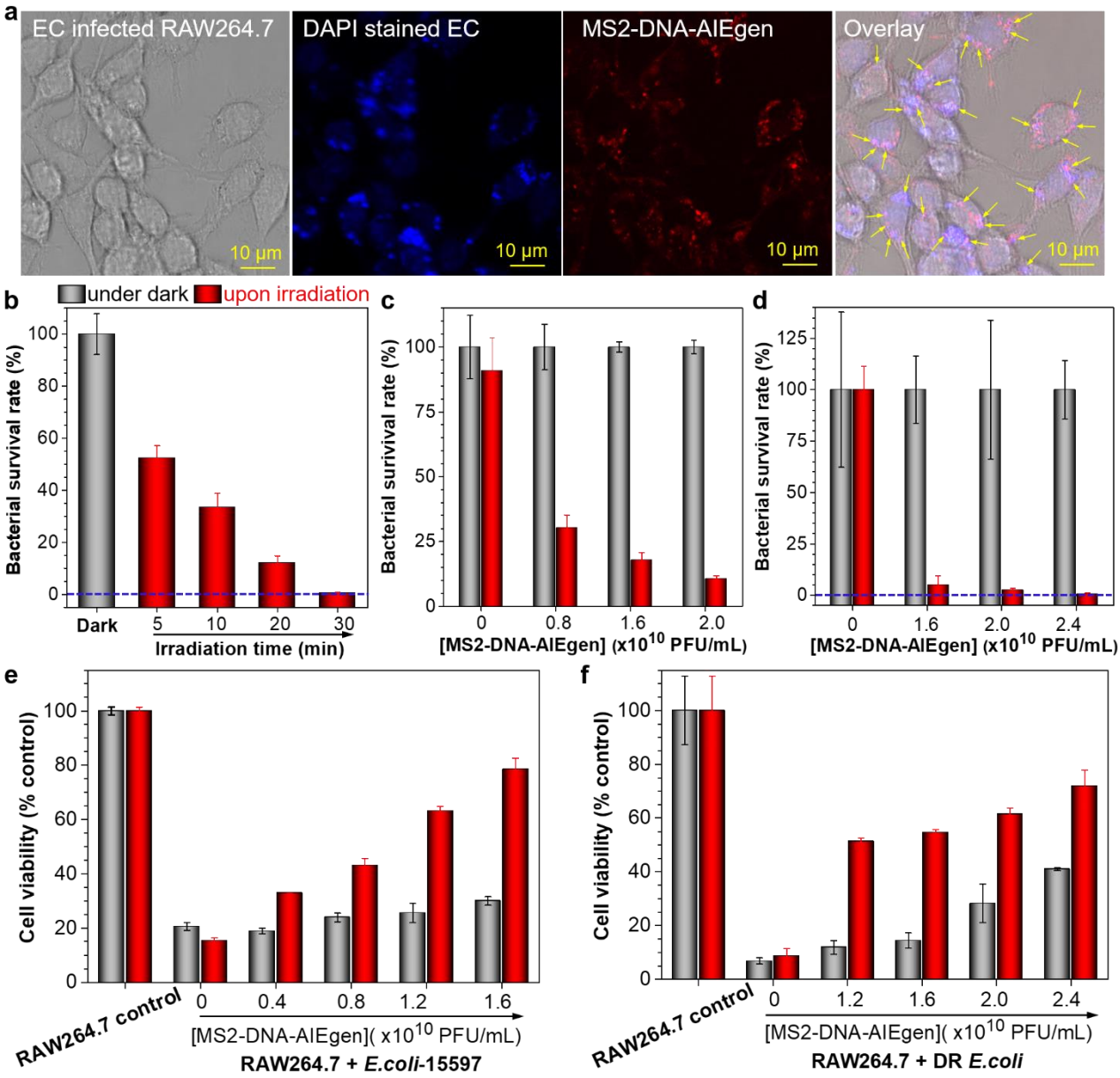

Figure 4. Targeting and elimination of intracellular bacterial infection. (a) Confocal imaging of RAW264.7 macrophages after infection by host *Escherichia coli*-15597 (stained by blue-color DAPI) treatment by MS2-DNA-AIEgen conjugates (red-color emission), sequentially. The arrows indicated the overlapped bacteria and MS2-DNA-AIEgen conjugates that showed purple color. (b) The calculated survival rate of host *Escherichia coli*-15597 extracted from RAW264.7 macrophages after treatment by MS2-DNA-AIEgen conjugates and sequentially different irradiation times. The blue dashed line indicated the 100% bacterial killing efficiency. (c) The calculated survival rate of host *Escherichia coli*-15597 (2.0×10^6 CFU·mL^{-1}) extracted from RAW264.7 macrophages after treatment by different concentrations of MS2-DNA-AIEgen conjugates. (d) The calculated survival rate of host DR-type *Escherichia coli*-001 (0.5×10^6 CFU·mL^{-1}) extracted from RAW264.7 macrophages after treatment by different concentrations of MS2-DNA-AIEgen conjugates. The blue dashed line indicated the 100% bacterial killing efficiency. (e) and (f) Cell viability test of macrophages RAW264.7 infected by host *Escherichia coli*-15597 and DR-type host *Escherichia coli*-001, respectively. The infected RAW264.7 cells were co-incubated with various concentrations of MS2-DNA-AIEgen conjugates for 1 hour, and then treated by white light irradiation or darkness for another 30 min.

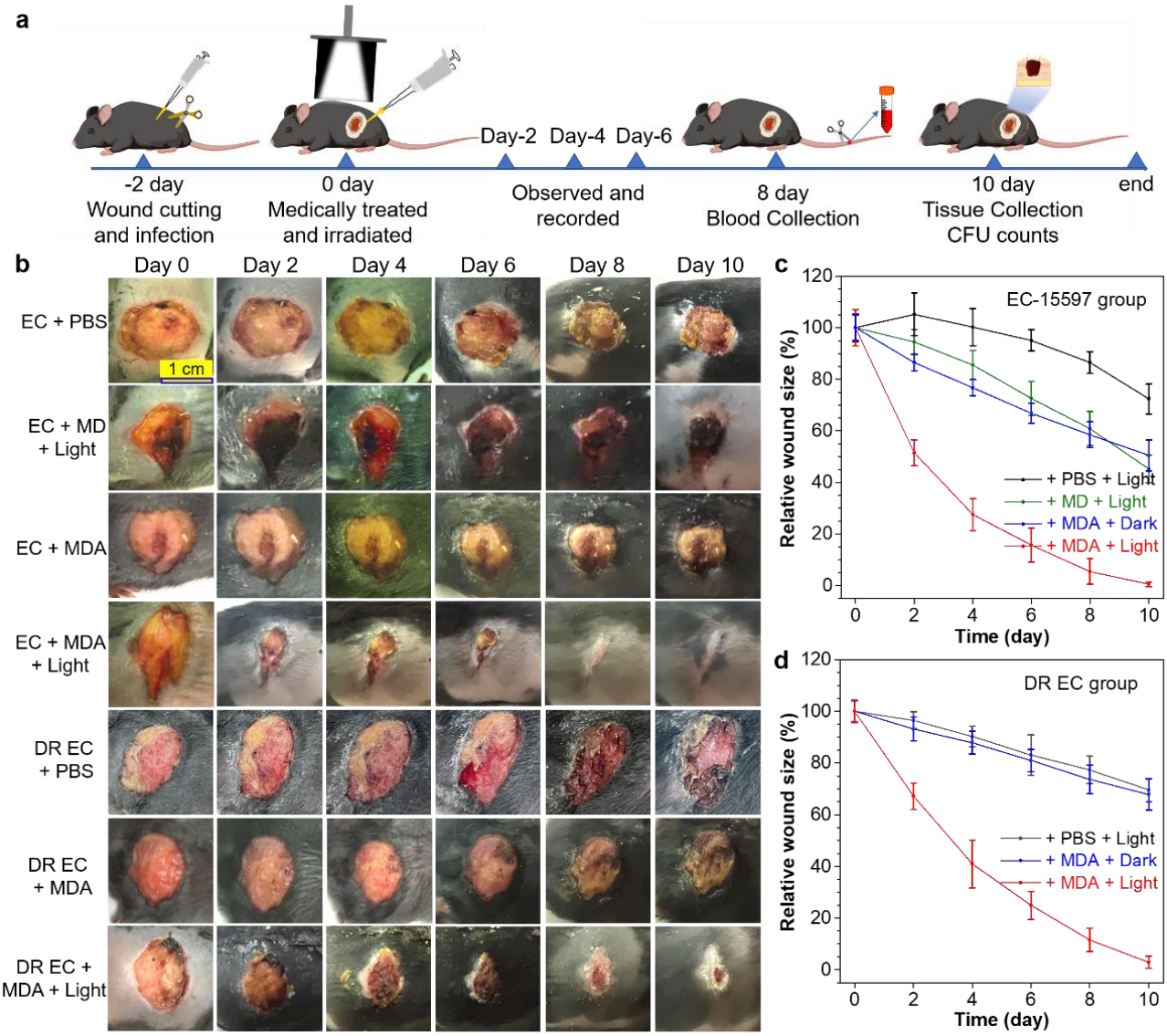

Figure 5. In vivo evaluation of antibacterial efficiency and wound healing rate of MS2-DNA-AIEgen bioconjugates against host *Escherichia coli*-15597 and DR-type host *Escherichia coli*-001 infected diabetic mice. (a) The treatment process on diabetic mice is illustrated with time elapsing. (b) Photographs of wounds change after different treatments. MS2-DNA-AIEgen was abbreviated as MDA. (c) Relative wound size analysis after host *Escherichia coli*-15597 infection and diverse treatments for 10 days. (d) Relative wound size analysis after DR-type host *Escherichia coli*-001 infection and diverse treatments for 10 days. The initial concentration of both above bacteria was 1.0×10^9 CFU·mL^{-1}.

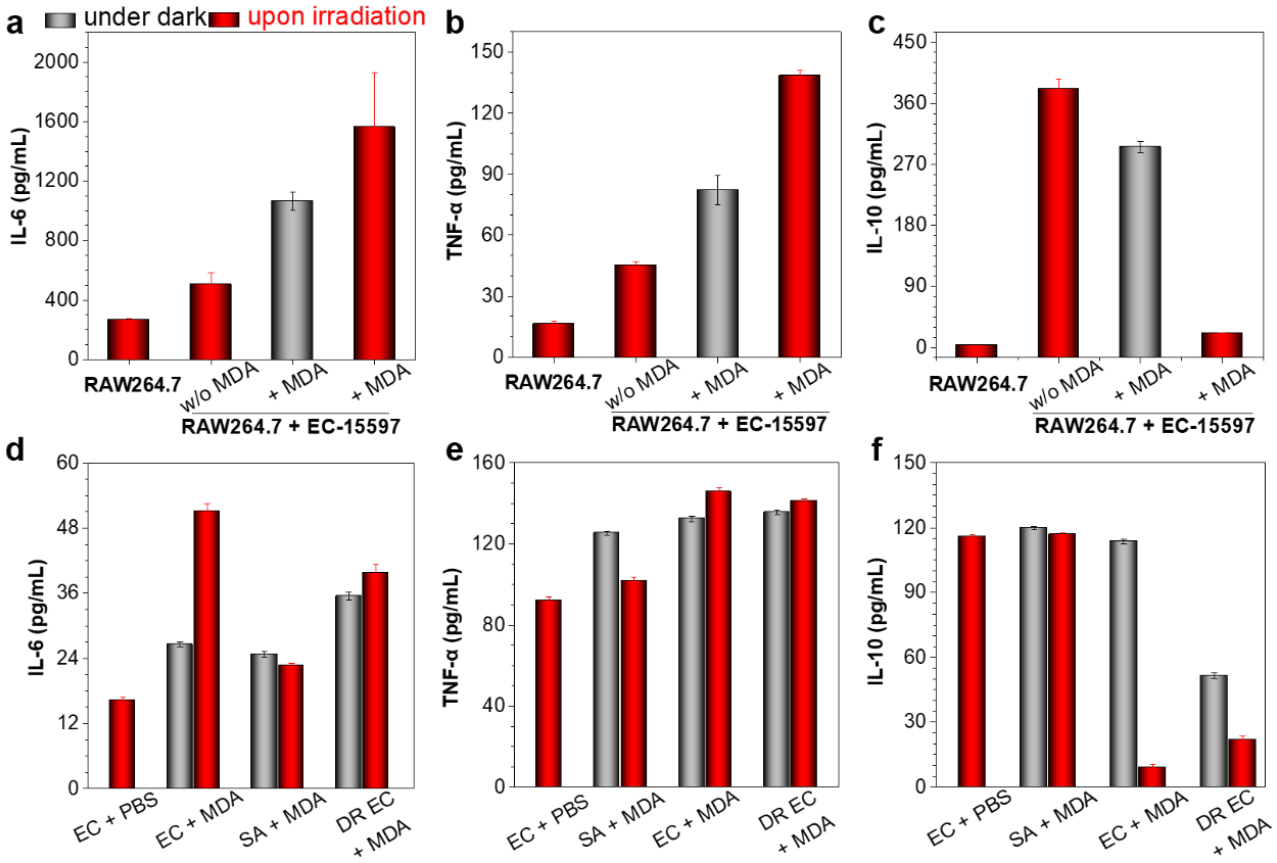

Figure 6. In vitro and in vivo antimicrobial immune response analysis. In vitro assay of the immune activation-related cytokines of (a) IL-6, (b) TNF-α, and immunosuppressive factor of (c) IL-10 in RAW264.7 macrophages before and after *Escherichia coli*-15597 infection and sequentially treated by MS2-DNA-AIEgen conjugates. (d-f) The corresponding change of immune-related factors in the venous blood of diabetic mice after bacterial infection and sequentially different treatments. w/o meant without; MDA was the abbreviation of MS2-DNA-AIEgen.